

# Three-dimensional facial volume analysis using algorithm-based personalized aesthetic templates

A. Jorien Tuin<sup>a</sup>, Jene W. Meulstee<sup>b</sup>,  
 Tom G. J. Loonen<sup>b</sup>, Joep Kraeima<sup>a</sup>,  
 Fred K. L. Spijkervet<sup>a</sup>,  
 Arjan Vissink<sup>a</sup>, Johan Jansma<sup>a</sup>,  
 Rutger H. Schepers<sup>a</sup>

<sup>a</sup>Department of Oral and Maxillofacial Surgery, University Medical Center Groningen, University of Groningen, Groningen, The Netherlands; <sup>b</sup>Department Oral and Maxillofacial Surgery, Radboud University Medical Center, Radboud University, Nijmegen, The Netherlands

A. Jorien Tuin, Jene W. Meulstee, Tom G. J. Loonen, Joep Kraeima, Fred K. L. Spijkervet, Arjan Vissink, Johan Jansma, Rutger H. Schepers: Three-dimensional facial volume analysis using algorithm-based personalized aesthetic templates. *Int. J. Oral Maxillofac. Surg.* 2019; xxx: xxx–xxx. © 2020 International Association of Oral and Maxillofacial Surgeons. Published by Elsevier Ltd. All rights reserved.

**Abstract.** Three-dimensional stereophotogrammetry is commonly used to assess volumetric changes after facial procedures. A lack of clear landmarks in aesthetic regions complicates the reproduction of selected areas in sequential images. A three-dimensional volumetric analysis was developed based on a personalized aesthetic template. The accuracy and reproducibility of this method were assessed. Six female volunteers were photographed using the 3dMDtrio system according to a clinical protocol, twice at baseline (T1) and twice after 1 year (T2). A styrofoam head was used as control. A standardized aesthetic template was morphed over the baseline images of the volunteers using a coherent point drift algorithm. The resulting personalized template was projected over all sequential images to assess surface area differences, volume differences, and root mean square errors. In 12 well-defined aesthetic areas, mean average surface area and volume differences between the two T1 images ranged from  $-7.6 \text{ mm}^2$  to  $10.1 \text{ mm}^2$  and  $-0.11 \text{ cm}^3$  to  $0.13 \text{ cm}^3$ , respectively. T1 root mean square errors ranged between 0.24 mm and 0.62 mm (standard deviation 0.18–0.73 mm). Comparable differences were found between the T2 images. An increase in volume between T1 and T2 was only observed for volunteers who gained in body weight. Personalized aesthetic templates are an accurate and reproducible method to assess changes in aesthetic areas.

**Key words:** 3D; stereophotogrammetry; template; coherent point drift; facial volume analysis.

Accepted for publication 14 January 2020

## Introduction

Three-dimensional (3D) stereophotogrammetry is commonly used to assess volumetric changes after facial aesthetic

procedures, e.g., fat grafting or fillers. Multiple 3D camera systems are available which are accurate up to  $0.2 \text{ mm}^{1,2}$ . However, the clinical accuracy of 3D stereophotogrammetry is limited due to

additional errors in the process, for example the matching and analysis of the 3D images and patient-related errors such as variations in facial expression or body weight<sup>3–5</sup>.

To objectify volume changes in a specific area of the face, 3D images need to be analysed by software systems. With existing software systems based on manual selection using brush or lasso tools, it is difficult to reproduce the exact same target area on sequential images, especially in areas without reproducible landmarks (cheeks or jowls)<sup>5-7</sup>. It becomes even more complicated when this target area has undergone changes, such as after fat grafting or fillers. This uncertainty has to be reduced to a minimum to allow for reliable comparison of sequential postoperative images with preoperative images and comparison of volume differences between different patients<sup>7-9</sup>.

To obtain better reproducible areas on 3D images after aesthetic facial procedures, we developed a method to measure volumetric changes in well-defined aesthetic areas using a personalized aesthetic template. The aim of this study was to assess the measurement error of a 3D volumetric analysis based on the personalized aesthetic template, as well as to assess its reproducibility when applied to sequential images of the volunteers after 1 year.

## Methods

A prospective study was designed in the departments of oral and maxillofacial surgery of the University Medical Center Groningen, Groningen, and the Radboud University Medical Center, Nijmegen, in

the Netherlands. The study was approved by the Medical Ethics Review Board of the University Medical Center Groningen protocol No. 201400179.

## Subjects and control

A rigid, non-deformable styrofoam 3D head (mannequin) was used as a control for the measurement error of the 3dMDtrio System (3dMD, Atlanta, GA, USA) and the software analysis. The mannequin was put in a fixed position in front of the 3D cameras for 26 photo series. Every photo series included one 3D image at baseline (1A) and one 3D image directly after the first image session, without a change in position (1B).

Six female volunteers without facial deformities were then asked to participate. 3dMD images were captured following a newly developed clinical 3D photo protocol for this purpose, with two photo sessions at baseline (T1, images 1A and 1B) and two sessions after 1 year (T2, images 2A and 2B). The second photo session (B) occurred directly after the first photo session (A) at baseline and after 1 year. Five photographs were taken per session: one test photo without instructions in order to get used to the environment and the flash of the camera. After this, four photos were taken with the instruction ‘‘relax your face, open your eyes and close your lips gently’’. The best fit image of every session, based on intended facial expression criteria, was chosen by two observers and

used for the analysis (AJT, TL). In the case of disagreement, a third observer (JM) gave a binding verdict. Each volunteer’s body weight was measured at T1 and T2 to ensure that the measured volume changes were not as a result of weight gain or loss.

## Creation of the personalized aesthetic template and analysis

### Preparation of 3D images

First, a standardized template (Fig. 1, Video 1) with 12 aesthetic regions per facial half was designed using Meshmixer 3D software (Autodesk Inc., San Francisco, CA, USA). Second, the standardized aesthetic template was globally aligned with all the selected images of the subject using seven globally pointed landmarks. Five landmarks (pupil left/right, nasion, labial commissure left/right) were located on every 3D image using the MATLAB v2017a (The Mathworks Inc., Natick, MA, USA) automatic landmark detection program<sup>10</sup>. Two additional landmarks were located manually on the baseline image by two observers (AJT, TGJL) at the most dorsal point of the skin surface at the frontozygomatic suture left and right using Vultus software (3dMD, Atlanta, GA, USA). The outer boundary of the personalized aesthetic template was applied to cut off and discard irrelevant regions of all 3D images.

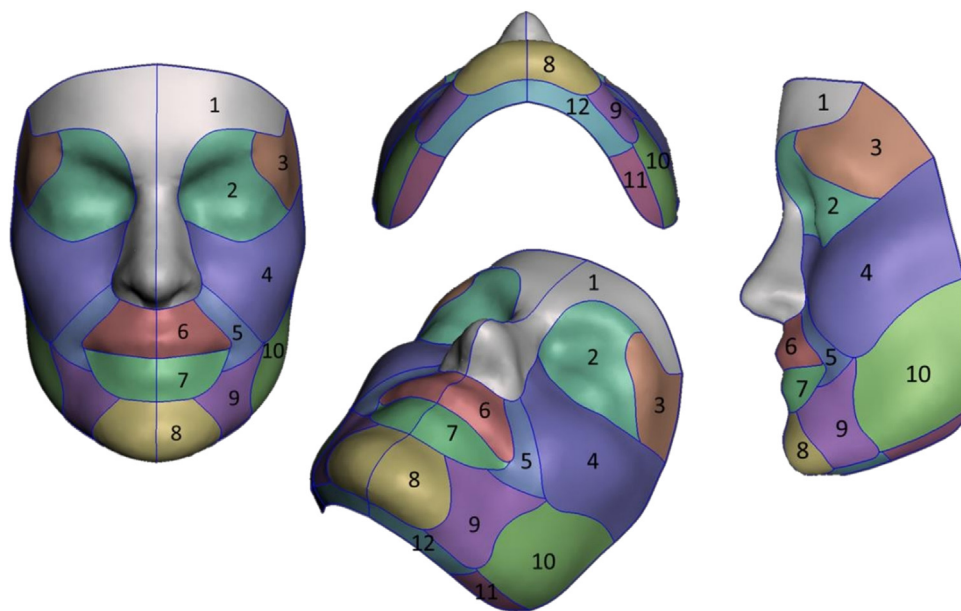


Fig. 1. Standard aesthetic template with 12 areas per facial half: 1, forehead/nose; 2, eye; 3, temporal area; 4, zygomatic area/cheeks; 5, nasolabial area; 6, upper lip; 7, lower lip; 8, chin; 9, prejowl area; 10, mandibular angle area; 11, submandibular area; 12, submental area.

### Application of the personalized aesthetic template

A non-rigid transformation based on coherent point drift (CPD) morphed the standardized aesthetic template towards the baseline 3D image (Supplementary Material Video 1)<sup>11</sup>. The CPD is an algorithm that is based on the spatial transformation of one set of points (template) to another existing set of points (3D image). CPD was set to 300 iterations and 200 degrees of freedom. The previously located landmarks were used to enhance the CPD algorithm with landmark guidance<sup>12</sup>. Using a ray casting algorithm, the corresponding points of all the template vertices were located on the corresponding 1A, 1B, 2A, and 2B images. As a result, 24 aesthetic areas were selected on every 3D image (Fig. 2). The forehead and nose regions were used to perform a second more accurate surface registration to match the baseline with the sequential images, since they are subject to less variation and are not so likely to be involved in most aesthetic facial procedures (fat grafting, fillers, face lift)<sup>4</sup>.

### Volume measurements

3D stereophotogrammetry results in a 3D image (a shell) without a volume; therefore an additional step was performed in MATLAB to assess volume differences between two 3D images. To calculate the volumes of the different aesthetic areas, a virtual backplane (reference backplane) was created by moving a copy of the baseline image (1A) 2 mm posterior in the direction of the point of gravity (Fig. 3) to prevent overlap between the tested images. This results in a space between the reference backplane and the 1A, 1B, 2A, and 2B images. Closing the borders between the 3D image and the corresponding reference backplane resulted in a bounded volume. Volume calculations were performed for every aesthetic zone in all images. All images used the same backplane (copy of 1A).

To verify the quality of the system and the software after 1 year (T2), a quality sub-analysis with the 3D images after 1 year (2A and 2B) was performed using 2A as a personalized aesthetic template and reference backplane.

### Data analysis

The alignment of all personalized templates (mannequin and volunteers) was checked by two observers (AJT, TL). The aesthetic personalized template of the mannequin was projected onto image 1A and 1B, and the volunteers' aesthetic personalized templates were projected onto images 1A, 1B, 2A, and 2B. Differences in surface area of the aesthetic areas were calculated. The volumes of the 1B, 2A, and 2B aesthetic areas were subtracted from the 1A volume to calculate volume differences compared to baseline (1A). The root mean square (RMS) error was calculated by dividing the volume difference by the surface area, resulting in a measurement error per aesthetic area in millimetres.

$$RMS\ error = \sqrt{\left(\frac{Volume\ difference}{Area}\right)^2}$$

### Statistical analysis

A descriptive analysis was performed on the surface area differences, volume



Fig. 2. Example of the application of the personalized template on four different 3D images of a test person.

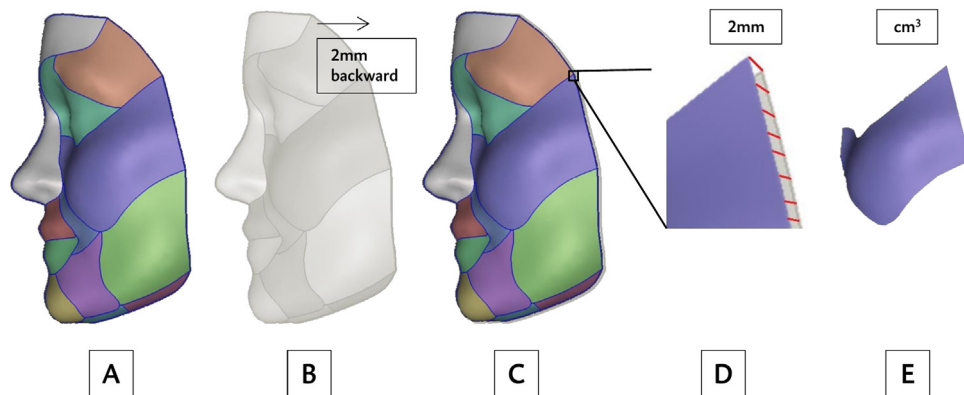


Fig. 3. Schematic illustration of volume calculations using the personalized aesthetic template. (A) 3D image with personalized aesthetic template. (B) The reference plane, which is a copy of the baseline images moved 2 mm backwards. (C) All sequential 3D images are projected onto the reference plane. (D) The borders of the 3D images and the reference plane are closed resulting in a bounded volume per aesthetic area. (E) Volume calculations are performed per aesthetic area.

differences, and RMS errors for each aesthetic area of the mannequin and the volunteers at baseline using IBM SPSS Statistics, version 23.0 (IBM Corp., Armonk, NY, USA). A Wilcoxon signed ranked test was applied for quality sub-analysis of the system at the different time points. For the assessment of measured differences between the two images of each individual aesthetic area at T2 (2A and 2B) compared to baseline, a Wilcoxon signed rank test was also performed.

**Results**

**Measurement error of the system and analysis**

No visible problems, such as wrongly projected or faulty discarded irrelevant regions of the template, were encountered with the automatic application of the aesthetic template to the baseline image of the styrofoam head. The average surface areas, volume differences, and RMS errors are given in Table 1A.

**Validation of the clinical protocol with female volunteers**

*Results at T1*

The demographic characteristics of the six female volunteers are given in Table 2. The average surface area differences, volume differences, and RMS errors ranged between -7.6 mm<sup>2</sup> and 10.0 mm<sup>2</sup> (SD 3.9–89.3 mm<sup>2</sup>), -0.11 cm<sup>3</sup> and 0.13 cm<sup>3</sup> (SD 0.19–2.91 cm<sup>3</sup>), and 0.24 mm and 0.64 mm (SD 0.18–0.73 mm), respectively, meaning that any differences caused by physical movements were limited and were comparable to the styrofoam head (Table 1B). Relatively low surface area deviations (SD < 2%) were seen in the nasolabial area, the zygoma/cheek area, and the lower lip. In general, the standard deviations of the surface area and volume differences were larger in the aesthetic areas with a greater surface area, such as the zygoma/cheek and forehead/nose. When the volume differences were corrected for the surface area (RMS error), the measurement errors between the different aesthetic areas were comparable.

*Results at T2*

The same analysis method as at T1 was used for quality sub-analysis of the system at T2. Average volume differences between baseline (1B versus 1A) and 1 year (2B versus 2A) were comparable (P = 0.660). There were no significant differences between the measured volume differences of images 2A and 2B compared to the baseline image (1A), when using the baseline image (1A) for backplane and template (P = 0.122).

*Differences between T1 and T2*

The overall volume difference in all aesthetic areas increased from 0.01 cm<sup>3</sup> at baseline to 0.50 cm<sup>3</sup> after 1 year. To find an explanation for this difference, an additional analysis was performed. An increase in volume was observed in three volunteers who had gained 2 kg in body weight between T1 and T2 (Table 1C and Table 1D, Table 2), while the body weight and volume difference of the other three volunteers was stable. The average volume difference after 1 year was 0.92 cm<sup>3</sup>

Table 1A. Results for the mannequin at T1 (1B).

	Count	Area (mm <sup>2</sup> )	Δ Area (mm <sup>2</sup> )	SD	% area Δ	SD	Δ Volume (cm <sup>3</sup> )	SD	RMS error (mm)	SD
1. Forehead/nose	52	3302	7.08	82.33	0.21	2.51	0.28	2.38	0.55	0.45
2. Eye	52	1301	0.69	9.51	0.05	0.74	0.05	0.54	0.33	0.26
3. Temporal	52	1405	0.81	34.43	0.10	2.36	0.02	1.00	0.55	0.42
4. Zygomatic/cheeks	52	3676	1.85	40.82	0.05	1.12	0.13	2.12	0.47	0.33
5. Nasolabial	52	509	-0.11	10.81	-0.03	2.06	0.04	0.49	0.69	0.66
6. Upper lip	52	648	5.77	23.94	0.89	5.41	0.08	0.71	0.74	0.70
7. Lower lip	52	567	-3.28	5.84	-0.57	4.97	0.06	0.47	0.59	0.57
8. Chin	52	929	-0.62	20.49	-0.10	2.24	0.05	0.89	0.73	0.59
9. Prejowl	52	1004	0.10	20.60	0.02	2.06	0.01	0.84	0.69	0.45
10. Mandibular angle	52	2151	12.30	43.42	0.59	1.02	0.06	1.28	0.48	0.33
11. Submandibular	52	404	9.57	20.22	2.26	3.66	0.10	0.76	1.46	1.63
12. Submental	52	230	4.23	11.32	1.98	2.15	0.06	0.76	2.55	1.87

Δ, difference; %, percentage; RMS, root mean square; SD, standard deviation.

Table 1B. Results for the six volunteers at T1 (1B).

	Count	Area (mm <sup>2</sup> )	Δ Area (mm <sup>2</sup> )	SD	% area Δ	SD	Δ Volume (cm <sup>3</sup> )	SD	RMS error (mm)	SD
1. Forehead/nose	12	4060	-1.11	89.30	-0.03	2.21	-0.04	2.32	0.45	0.35
2. Eye	12	1693	10.05	20.71	0.64	1.34	-0.01	0.49	0.24	0.18
3. Temporal	12	1800	-1.65	47.08	-0.08	2.66	0.11	1.44	0.64	0.46
4. Zygomatic/cheeks	12	4037	-3.74	68.23	-0.10	1.67	0.12	2.91	0.56	0.39
5. Nasolabial	12	521	2.37	3.85	0.44	0.73	-0.01	0.28	0.42	0.28
6. Upper lip	12	621	-1.86	14.39	-0.42	2.31	-0.04	0.24	0.31	0.26
7. Lower lip	12	490	-0.75	6.24	-0.22	1.18	-0.06	0.19	0.25	0.29
8. Chin	12	793	-7.63	27.56	-0.96	3.32	-0.11	0.36	0.33	0.33
9. Prejowl	12	908	-0.19	21.48	-0.11	2.30	-0.01	0.56	0.48	0.34
10. Mandibular angle	12	2195	1.43	57.42	0.04	2.52	0.13	1.87	0.64	0.45
11. Submandibular	12	325	1.76	6.91	0.70	2.30	0.02	0.25	0.62	0.73
12. Submental	12	341	-0.64	5.41	-0.23	1.59	0.01	0.20	0.43	0.37

Δ, difference; %, percentage; RMS, root mean square; SD, standard deviation.

Table 1C. Results for the three volunteers without a weight change at T2 (2A and 2B).

	Count	Area (mm <sup>2</sup> )	Δ Area (mm <sup>2</sup> )	SD	% area Δ	SD	Δ Volume (cm <sup>3</sup> )	SD	RMS error (mm)	SD
1. Forehead/nose	12	3975	42.92	111.29	1.22	2.88	1.28	2.99	0.65	0.48
2. Eye	12	1666	4.17	9.25	0.26	0.55	0.05	0.58	0.29	0.18
3. Temporal	12	1712	0.36	32.80	0.04	1.96	0.05	0.93	0.41	0.35
4. Zygomatic/cheeks	12	3905	-18.58	45.35	-0.48	1.21	-0.50	1.91	0.40	0.30
5. Nasolabial	12	496	0.66	10.16	0.06	1.94	0.10	0.24	0.43	0.30
6. Upper lip	12	615	12.61	17.62	2.08	2.93	0.09	0.25	0.35	0.21
7. Lower lip	12	477	7.17	12.56	1.61	2.98	0.05	0.18	0.32	0.18
8. Chin	12	758	0.86	32.52	-0.01	4.59	0.10	0.28	0.29	0.26
9. Prejowl	12	873	2.36	17.27	0.13	2.05	0.13	0.37	0.39	0.24
10. Mandibular angle	12	2122	-10.69	38.07	-0.58	1.81	-0.40	1.07	0.46	0.28
11. Submandibular	12	283	0.35	11.00	0.20	4.45	-0.03	0.23	0.66	0.45
12. Submental	12	329	-9.70	16.78	-2.92	5.02	-0.07	0.27	0.68	0.51

Δ, difference; %, percentage; RMS, root mean square; SD, standard deviation.

Table 1D. Results for the three volunteers with a weight change at T2 (2A and 2B).

	Count	Area (mm <sup>2</sup> )	Δ Area (mm <sup>2</sup> )	SD	% area Δ	SD	Δ Volume (cm <sup>3</sup> )	SD	RMS error (mm)	SD
1. Forehead/nose	12	4357	124.44	189.16	2.86	4.45	5.48	6.20	1.57	0.91
2. Eye	12	1728	20.00	15.38	1.17	0.88	0.37	1.13	0.58	0.33
3. Temporal	12	1967	81.16	138.36	3.97	6.98	1.98	2.96	1.24	0.96
4. Zygomatic/cheeks	12	4179	19.12	116.97	0.44	2.68	1.67	4.21	0.78	0.63
5. Nasolabial	12	539	3.18	19.85	0.71	3.84	0.22	0.48	0.78	0.54
6. Upper lip	12	667	10.50	37.67	1.70	5.59	0.20	0.52	0.70	0.43
7. Lower lip	12	501	-6.49	9.39	-1.23	1.79	0.02	0.34	0.56	0.38
8. Chin	12	850	11.30	45.19	1.35	5.46	0.20	0.58	0.57	0.39
9. Prejowl	12	951	9.23	29.30	1.00	3.04	0.33	0.82	0.66	0.60
10. Mandibular angle	12	2261	6.12	70.47	0.29	2.98	0.31	2.25	0.60	0.68
11. Submandibular	12	396	19.07	46.00	5.69	14.16	0.18	0.43	0.75	0.80
12. Submental	12	348	8.33	14.04	2.60	4.25	0.12	0.29	0.66	0.58

Δ, difference; %, percentage; RMS, root mean square; SD, standard deviation.

for the volunteers who had a weight gain and 0.07 cm<sup>3</sup> for those who had not.

## Discussion

This study introduced a new and accurate 3D analysis method to evaluate sequential 3D images, based on personalized aesthetic templates. The use of this designed 3D clinical photo protocol to reduce the influence of physiological differences, such as facial expression, resulted in volume differences that were comparable to those obtained with a styrofoam head.

With this 3D technique, measurement errors are an accumulation of errors of 3D photo acquisition, template projection, and matching of the 3D surfaces. Moreover, physiological differences in the face can influence the variation in measurements. RMS errors are often used to evaluate measurement errors, because absolute volume differences are dependent on the size of the selected area. A study by Maal et al. on the accuracy of 3D stereophotogrammetry found a variation of 0.25 mm (0.21–0.27 mm) based on 100 images of one person<sup>4</sup>. An additional variation of approximately 0.15 mm was found over

6 weeks. The present study did not show additional variation after 1 year. In our opinion, the selection of different photos and following strict instructions minimize the influence of facial expression over time. However, the variation reported by Maal et al. was still lower after 6 weeks than our RMS error variation after 1 year, which was 0.29–0.68 mm. In the study of Maal et al., only one person was used for 100 3D photos. The use of a single test person might explain the lower RMS error, because in another study, Maal et al. found higher variations in a clinical test group of 15 volunteers of around 0.5 mm RMS error after 3 weeks<sup>3</sup>. The results of this clinical test group were comparable to our results.

This study is novel in using an individualized template to automatically determine specific aesthetic regions on sequential images from the same person. The personalized aesthetic template method was designed to replace the rather inaccurate lasso or brush tool method to encircle target aesthetic areas manually on sequential images. Many previous clinical studies that have evaluated aesthetic facial

Table 2. Demographic characteristics of the test persons.

	Gender (M/F)	Age (years)	Height (cm)	Weight T1 (kg)	BMI T1 (kg/m <sup>2</sup> )	Weight T2 (kg)
1	F	63	178	79	24.9	79
2	F	27	172	58	19.6	58
3	F	27	177	70	22.3	72
4	F	44	180	70	21.6	72
5	F	43	173	75	25.1	77
6	F	26	175	68	22.2	68

BMI, body mass index; M, male; F, female.

procedures using 3D imaging have had inaccuracies in the encircled areas at different time points<sup>6–8</sup>. Manual selection of the target area could result in selection bias and unreliable volumetric outcomes. In this study, there was no human interference (and potential selection bias) in the selection of the aesthetic areas. Moreover, especially in regions without obvious landmarks, such as the zygoma/cheek and nasolabial area, this technique showed the smallest variation in surface area differences after 1 year.

The projection of the aesthetic template onto the 3D image was performed using an algorithm based on the CPD<sup>11</sup>. This algorithm uses the coherent movement of surface points (standard aesthetic template) to other surface points (baseline image) in order to preserve the topological structure of the template. Since the algorithm is based on this CPD and uses a total set of points of a standard model instead of only a few landmarks, the assumption is that the template will, at the least, also suit faces with minor deformities (mild craniofacial microsomia, after trauma, minor scarring). The advantage of algorithm-based personalized templates is that volumetric changes, especially in regions without clear landmarks, can be compared objectively between patients.

The clinical 3D photo protocol used in this study included instructions to relax the facial expression, which is known to be the most reproducible one<sup>13</sup>. In order to reduce the effect of facial expression even more, the best image of the session was used. The protocol measurement errors were comparable to those attained with a fixed styrofoam head. Although we have previously stated that we prefer to keep inaccuracies caused by human intervention as low as possible, this selection step has not been automated yet. No software programs or algorithms are available that are as good as the human eye to determine subtle differences in facial expression. Hence, human intervention remains unavoidable for the selection of the images.

In conclusion, a new 3D protocol to evaluate 3D images reliably, based on personalized aesthetic templates, was introduced and tested. This is an accurate automated method to evaluate specific aesthetic areas of the face. Measurement

errors comparable to those obtained with a styrofoam head were achieved using the developed clinical 3D photo protocol by focusing on the standardization of facial expression.

#### Patient consent

The publication of the photographs and video material was approved by the test person.

#### Funding

No funding was received for this manuscript.

#### Ethical approval

The study was approved by the Medical Ethics Review Board of the University Medical Center Groningen (protocol No. 201400179).

#### Competing interests

No competing interests.

#### Appendix A. Supplementary data

Supplementary material related to this article can be found, in the online version, at doi:<https://doi.org/10.1016/j.ijom.2020.01.013>.

#### References

- [1] Lubbers HT, Medinger L, Kruse A, Gratz KW, Matthews F. Precision and accuracy of the 3dMD photogrammetric system in craniomaxillofacial application. *J Craniofac Surg* 2010;**21**:763–7.
- [2] Verhulst A, Hol M, Vreeken R, Becking A, Ulrich D, Maal T. Three-dimensional imaging of the face: a comparison between three different imaging modalities. *Aesthet Surg J* 2018;**38**:579–85.
- [3] Maal TJ, van Loon B, Plooij JM, Rangel F, Ettema AM, Borstlap WA, Bergé SJ. Registration of 3-dimensional facial photographs for clinical use. *J Oral Maxillofac Surg* 2010;**68**:2391–401.
- [4] Maal TJ, Verhamme LM, van Loon B, Plooij JM, Rangel FA, Kho A, Bronkhorst EM, Bergé SJ. Variation of the face in rest using 3D stereophotogrammetry. *Int J Oral Maxillofac Surg* 2011;**40**:1252–7.
- [5] Rawlani R, Qureshi H, Rawlani V, Turin SY, Mustoe TA. Volumetric changes of the mid and lower face with animation and the standardization of three-dimensional facial imaging. *Plast Reconstr Surg* 2019;**143**:76–85.
- [6] van der Meer WJ, Dijkstra PU, Visser A, Vissink A, Ren Y. Reliability and validity of measurements of facial swelling with a stereophotogrammetry optical three-dimensional scanner. *Br J Oral Maxillofac Surg* 2014;**52**:922–7.
- [7] Schreiber JE, Turner J, Stern CS, Beut J, Jelks EB, Jelks GW, Tepper OM. The boomerang lift: a three-step compartment-based approach to the youthful cheek. *Plast Reconstr Surg* 2018;**141**:910–3.
- [8] Zhu M, Xie Y, Zhu Y, Chai G, Li Q. Response to comment on: A novel noninvasive three-dimensional volumetric analysis for fat-graft survival in facial recontouring using the 3L and 3M technique. *J Plast Reconstr Aesthet Surg* 2016;**69**:1161–2.
- [9] Sasaki GH. The safety and efficacy of cell-assisted fat grafting to traditional fat grafting in the anterior mid-face: an indirect assessment by 3D imaging. *Aesthetic Plast Surg* 2015;**39**:833–46.
- [10] Zhang K, Zhang Z, Li Z, Qiao Y. Joint face detection and alignment using multitask cascaded convolutional networks. *IEEE Signal Process Lett* 2016;**23**:1499–503.
- [11] Myronenko A, Song X. Point set registration: Coherent point drift. *IEEE Trans Pattern Anal Mach Intell* 2010;**32**:2262–75.
- [12] Hu Y, Rijkhorst E, Manber R, Hawkes D, Barratt D. Deformable vessel-based registration using landmark-guided coherent point drift. In: *Medical imaging and augmented reality*. Berlin, Heidelberg: Springer; 2010: 60–9.
- [13] Sawyer AR, See M, Nduka C. Assessment of the reproducibility of facial expressions with 3-D stereophotogrammetry. *Otolaryngol Head Neck Surg* 2009;**140**:76–81.

Corresponding author at: Department of Oral and Maxillofacial Surgery  
University Medical Center Groningen  
University of Groningen  
Postbus 30.001  
9700 RB Groningen  
The Netherlands  
E-mail: [a.j.tuin@umcg.nl](mailto:a.j.tuin@umcg.nl)